Synthesis and Stereosequence Distribution Analysis of poly (Styrene-co-Ethyl Acrylate) by NMR Spectroscopy

Puneeta Sarin[1], Deepika Khandelwal[2], Rama Kant Goyal[3], Geetu Gambhir[4], Manisha Verma[5], Sanjeeta Rani[6], Laishram Saya[7], Sunita Hooda[8]

[1]*Amity Global School, Noida, Uttar Pradesh, India.*

[2,8]*Polymer Research Laboratory, Department of Chemistry,*
Acharya Narendra Dev College, University of Delhi, New Delhi-110019, India.

[3]*Department of Chemistry, Ramjas College, University of Delhi, Delhi -110007.*

[4]*Advance Chemistry Research Laboratory, Department of Chemistry,*
Acharya Narendra Dev College, University of Delhi, New Delhi-110019, India.

[5,6]*Department of Physics, Acharya Narendra Dev College,*
University of Delhi, New Delhi-110019, India.

[7]*Department of Chemistry, Sri Venkateswara College,*
University of Delhi, Dhaula Kuan, New Delhi-110021, India

http://doi.org/10.64643/IJIRTV12I5-185732-459

Abstract— **Styrene/alkyl acrylate copolymers are widely used in commercial applications such as paints, adhesives, coatings, and packaging. They also play a crucial role in the automotive, electronics, and medical sectors. Their versatility is demonstrated by their use in binder applications, paper coatings, and as strengthening agents for kraft bagasse pulp. These copolymers are valued for their excellent water resistance and moisture vapor transmission rates, making them ideal for construction primers. Additionally, incorporating acrylate rubber into styrene-acrylonitrile copolymers improves weather, heat, and chemical resistance, making them suitable for outdoor applications. Research on styrene/alkyl acrylate copolymers has revealed important insights into their microstructure, with studies using NMR spectroscopy to analyze sequence distribution and polymerization kinetics. Recent work has focused on improving the characterization of these copolymers' properties using two-dimensional NMR techniques, offering a more detailed understanding of their structural and intermolecular properties. This study presents a detailed analysis of styrene/ethyl acrylate (S/E) copolymers using $^{13}C\{^1H\}$, DEPT, HSQC, TOCSY, and HMBC NMR spectroscopy. The copolymer was synthesized using atom transfer radical polymerization (ATRP), and its composition were determined by Gel Permeation Chromatography (GPC) and ^1H NMR spectroscopy. The Kelen-Tüdős (KT) method and the nonlinear error-in-variables approach (EVM) were used to calculate reactivity ratios.**

I. INTRODUCTION

Styrene/alkyl acrylate copolymers are economically viable materials with a wide range of commercial applications, particularly in paints, adhesives, and coatings. They are essential components in terpolymer systems, such as those used in wax production. These copolymers have seen significant growth in the packaging industry, enabling the creation of attractive containers, dinnerware, and bottle labels, while also expanding into the fast food, automotive, and electronics sectors, contributing to the production of devices like computers and telecommunication equipment. Furthermore, they have valuable applications in the medical field[1]. Copolymers of styrene were also used for 3d printable meterials[2]. Homo- and copolymers of acrylates are highly versatile and sought after in various industries due to their adaptability in copolymer compositions[3] and pendant groups. The addition of acrylates or methacrylates to styrene chains improves durability and raises the softening point. By incorporating a small amount of a second monomer into styrene, the resulting copolymer exhibits improved properties over traditional polystyrene, including higher softening

points and reduced brittleness. Research has also investigated styrene/methyl acrylate blends for curing polyester binders in smokeless propellant fuels, demonstrating improved performance[4].

The potential of styrene/acrylate emulsions as reinforcement agents for kraft bagasse pulp to enhance the mechanical strength of paper has been also explored by researchers. Xie P. et al. developed novel acrylate emulsions and investigated how their interaction with nanocellulose contributes to improved paper durability[5]. Additionally, studies have focused on the influence of styrene concentration on the tensile properties of styrene-acrylate films, revealing significant relationships between monomer composition and mechanical performance. Musa M. S. et al. examined these effects, emphasizing the role of styrene content in determining film strength[6].

Styrene-acrylic polymers are also valued for their superior water resistance and moisture vapor transmission rates (MVTR) compared to all-acrylic polymers, making them ideal for use in construction primers and paper coatings. Moreover, the incorporation of acrylate rubber into styrene-acrylonitrile copolymers results in materials like acrylonitrile styrene acrylate (ASA), which offer improved weather resistance, long-term heat resistance, and chemical resistance, making them suitable for automotive and outdoor applications[7]. These studies highlight the versatility and potential of styrene/alkyl acrylate copolymers, underscoring their growing importance across various industrial and technological sectors.

Chain Tacticity shows effect on the thermal conductivity of isotactic and syndiotactic polystyrene[8]. Several studies[9-19] have focused on the triad distribution and tacticity parameters of styrene/alkyl acrylate copolymers.

Doremale et al.[9] investigated the structure of styrene/methyl acrylate (S/M) using ^{1}H and $^{13}C\{^{1}H\}$ NMR spectroscopy. Similarly, Poehlein et al.[10] explored the sequence distribution of styrene/acrylic acid up to the triad level, validating their results using the Alfrey-Mayo model. Randall[11] investigated the configurational aspects of amorphous polystyrene, noting the influence of ring current effects on methylene carbon chemical shifts, primarily determined by adjacent phenyl substituents. He developed aromatic substituent parameters in conjunction with Grant and Paul's model to calculate chemical shifts in aromatic hydrocarbons and polymers. Koinuma et al.[12] analysed the $^{13}C\{^{1}H\}$ NMR spectra of styrene/methyl acrylate copolymers through modelling. Guillot et al.[13–14] produced styrene/ethyl acrylate copolymers using batch emulsion polymerization, and then investigated their polymerization kinetics and examining the microstructure concerning the glass transition temperature.

Guzman et al.[15] investigated the sequence distribution in styrene/butyl acrylate copolymers synthesized via emulsion polymerization, utilizing $^{13}C\{^{1}H\}$ NMR spectroscopy. Ito and Yamashita's[16] analysis led to the determination of cotacticity for random copolymers, differing from the alternating copolymers' expected value ($\sigma_{sm} = 0.5$). An alternative assignment suggested a lower cotacticity value ($\sigma_{sm} = 0.30$). Kobayashi[17] examined the effect of sequence distribution on the glass temperature of terpolymers and extended the modified Gibbs-DiMarzio equation, which was initially developed for binary copolymers, to be applicable to terpolymers.

Vander Boomen et al.[18] synthesized styrene/methyl acrylate copolymers using continuous emulsion polymerization, revealing strong compositional drift in batch copolymerization experiments. Hooda et al.[19-20] analysed the microstructure of styrene in terms of triad fractions and tacticity parameters, providing insights into their intramolecular structure.

The mechanical properties of vinyl polymeric materials are fundamentally influenced by their microstructure, particularly monomer sequence distribution[21-22]. The spectral patterns of copolymers are often complex, as chemical shifts are affected not only by sequence distribution but also by the stereochemical arrangement of monomeric units along the polymer chain.

NMR spectroscopy is a highly effective technique for examining the intramolecular structure, including sequence distribution and tacticity, as well as intermolecular properties in vinyl copolymers[23-25.] Conventional one-dimensional NMR methods often struggle with precise signal assignments. Consequently, two-dimensional NMR techniques have become the most effective method for accurately analyzing copolymer microstructure [26-32]. The effect of reaction temperature on tacticity in the polymerization of methyl methacrylate with the help of Nuclear

Magnetic Resonance Spectroscopy was done by Jozaghkar M. et al.[33].

This study provides a detailed characterization of styrene/ethyl acrylate (S/E) copolymer, examining its compositional and configurational sequences through $^{13}C\{^1H\}$, DEPT, HSQC, TOCSY, and HMBC NMR techniques. The copolymer was synthesized using atom transfer radical polymerization (ATRP)[34,35]. Gel Permeation Chromatography (GPC) analysis revealed that its molecular weight increased with higher conversion rates.

Copolymer composition was analyzed using ^1H NMR spectroscopy, and the data obtained was utilized to calculate reactivity ratios through KT[36] and EVM[37] methods. The microstructural analysis focused on the distribution of S- and E-centered triad sequences. To confirm the triad sequence distribution, both $^{13}C\{^1H\}$ NMR data and reactivity ratio calculations were employed.

The NMR spectra of the copolymer indicate that the methylene (CH_2) and methine (CH) signals are composition-dependent and exhibit significant overlap. Even Distortion less Enhancement by Polarization Transfer (DEPT) was unable to separate these overlapping signals. To precisely identify the different resonance signals, advanced techniques such as Single Quantum Coherence (HSQC), Total Correlation Spectroscopy (TOCSY), and Heteronuclear Multiple Bond Correlation (HMBC) were utilized.

II. EXPERIMENTAL

Styrene ('S') and Ethyl Acrylate ('E') from Aldrich were purified through distillation under reduced pressure and stored at temperatures < 7°C. HPLC-grade solvents, obtained from Aldrich, were used without further purification. All other chemicals were utilized in their received form.

A series of styrene/ethyl acrylate (S/E) copolymers was synthesized under ATRP conditions using varying molar ratios of [Monomer]: [MBP]: [CuBr]: [Cu (0)]: [PMDETA]: 200:0.3:1:1:1. Samples were collected at different time intervals to monitor changes in molecular weight during polymerization. The GPC analysis revealed a linear enhancement in molecular weight with conversion, while polydispersity remained narrow (1.12–1.28). Figure 1 illustrates this linear trend, confirming the polymerization process is well-controlled.

III. COPOLYMER COMPOSITION AND REACTIVITY RATIOS DETERMINATION

The proportional areas of the phenyl (S_1) and OCH_2 (S_2) proton signals were measured from the ^1H NMR spectrum, and the copolymer composition was subsequently determined using the following equation.

$F_S = [S_1/5] / [(S_1/5+S_2/2)]$

Where, the mole fraction of styrene (S) monomer in the copolymer is represented by Fs. The detailed composition data is shown in Table 1.

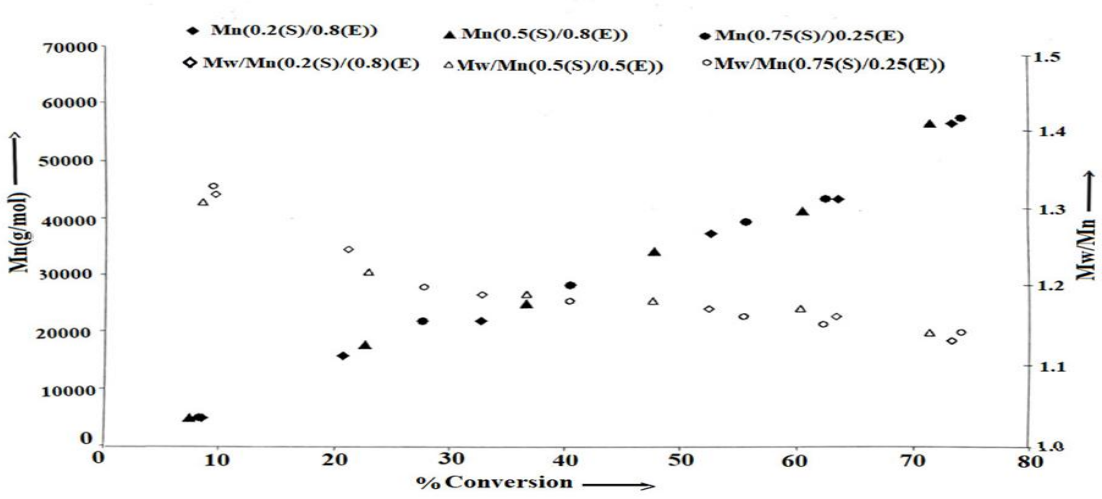

Figure 1. Variation of molecular weight and polydispersity with the conversion of S/E copolymers synthesized by ATRP.

Table 1: Copolymer composition data of the S/E copolymers (<10% conversion)

Sample No.	Styrene mole fraction infeed (f_S)	Styrene mole fraction in copolymer (F_S)
1.	0.20	0.30
2.	0.40	0.49
3.	0.50	0.58
4.	0.65	0.69
5.	0.80	0.80

The reactivity ratios were initially estimated using KT method, which yielded terminal model reactivity values of $r_S = 0.91 \pm 0.1$ and $r_E = 0.44 \pm 0.08$. These values were further refined using the nonlinear EVM approach, resulting in reactivity ratios of $r_S = 0.96$ and $r_E = 0.47$.

For all three feed compositions, the plot of F_S against the percentage of conversion (Figure 2) shows that the copolymer composition varies with conversion. The composition of the comonomer feed also shifts as the conversion progresses. As conversion increases, more ethyl acrylate integrates into the polymer chain, causing a shift toward the less reactive monomer.

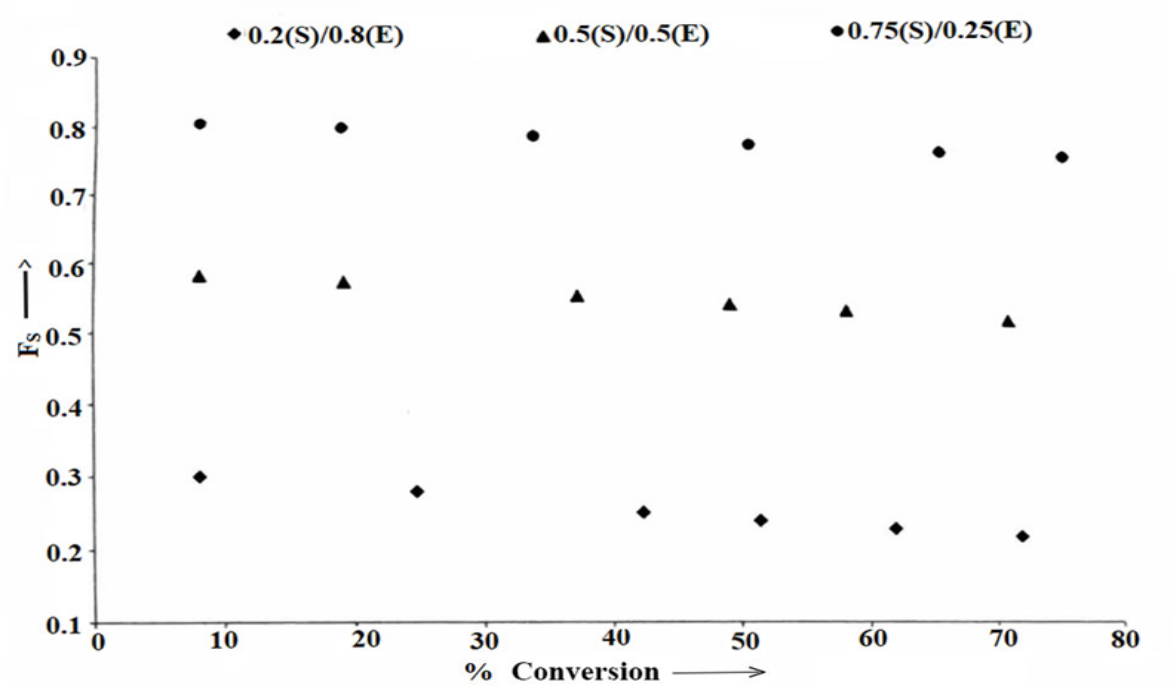

Figure 2. Variation of copolymer composition (F_s) as a function of conversion for the S/E copolymers

IV. ^{1}H NMR STUDIES

Figure 3 displays the assigned resonance signals in the ^{1}H NMR spectrum of the S/E copolymer with F_E = 0.49. The oxymethylene (OCH_2) proton resonances appearing as a split signal between δ 4.15–3.45 ppm, shows minimal sensitivity to stereochemical configuration in poly (ethyl acrylate). This splitting occurs due to the shielding effect of the phenyl ring in the S unit. Likewise, phenyl proton resonances appear as two distinct peaks around δ 6.79 ppm corresponding to the o-protons. The δ 1.15 and 2.50 ppm region is highly overlapped, tentatively attributed to CH and CH_2 protons of both E and S units.

The δ 0.55–1.15 ppm region corresponds to the methyl (CH_3) protons of the E unit. To distinguish overlapping signals and fully assign the ^{1}H NMR spectrum, a combination of 1D (DEPT, $^{13}C\{^1H\}$) and 2D (HSQC and TOCSY) NMR techniques was employed.

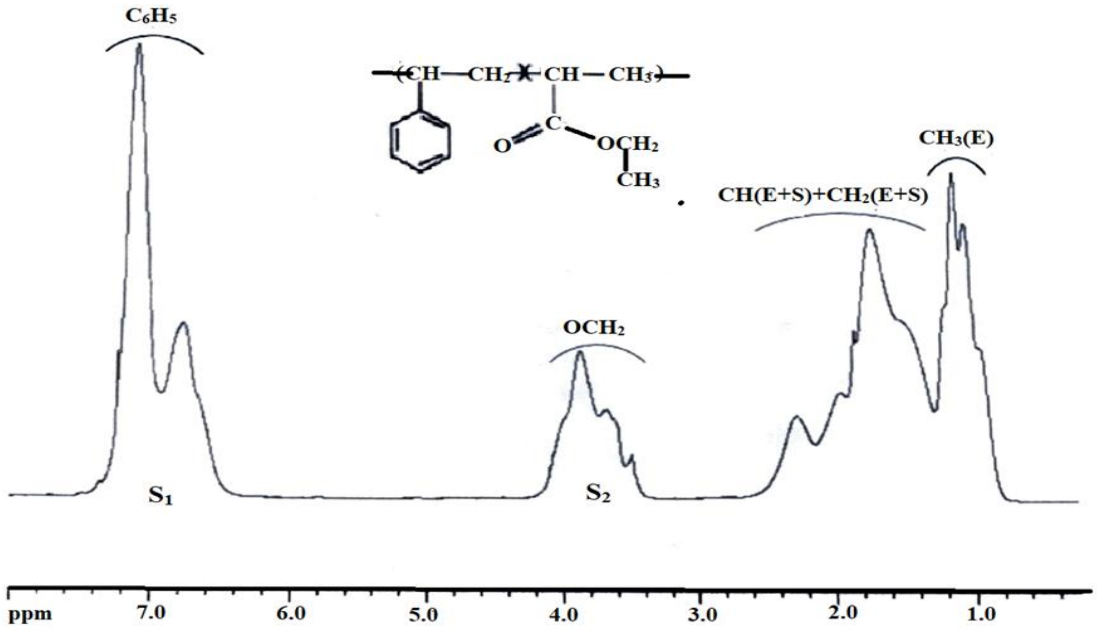

Figure 3. ^{1}H NMR spectrum of the styrene/ethyl acrylate copolymer ($F_S = 0.49$) in $CDCl_3$ at 25°C

V. $^{13}C\{^{1}H\}$ NMR STUDIES

Figure 4 illustrates the complete assignment of the $^{13}C\{^{1}H\}$ NMR spectrum for the S/E copolymer with $F_E = 0.49$. The assignments were determined by comparing this spectrum with those of the respective homopolymers, along with DEPT-135 and DEPT-90 spectra shown in Figure 5 and Figure 6 respectively.

The OCH_2 group of the E unit is detected at δ 61.40 ppm and remains unchanged by changes in composition or configuration. The spectral range between δ 34.45 and 48.78 ppm corresponds to the CH and CH_2 carbons of E and S units, though it exhibits significant overlap and complexity. In the DEPT-90 NMR spectrum, CH carbon signals from both units appear within the δ 37.23–41.18 ppm range.

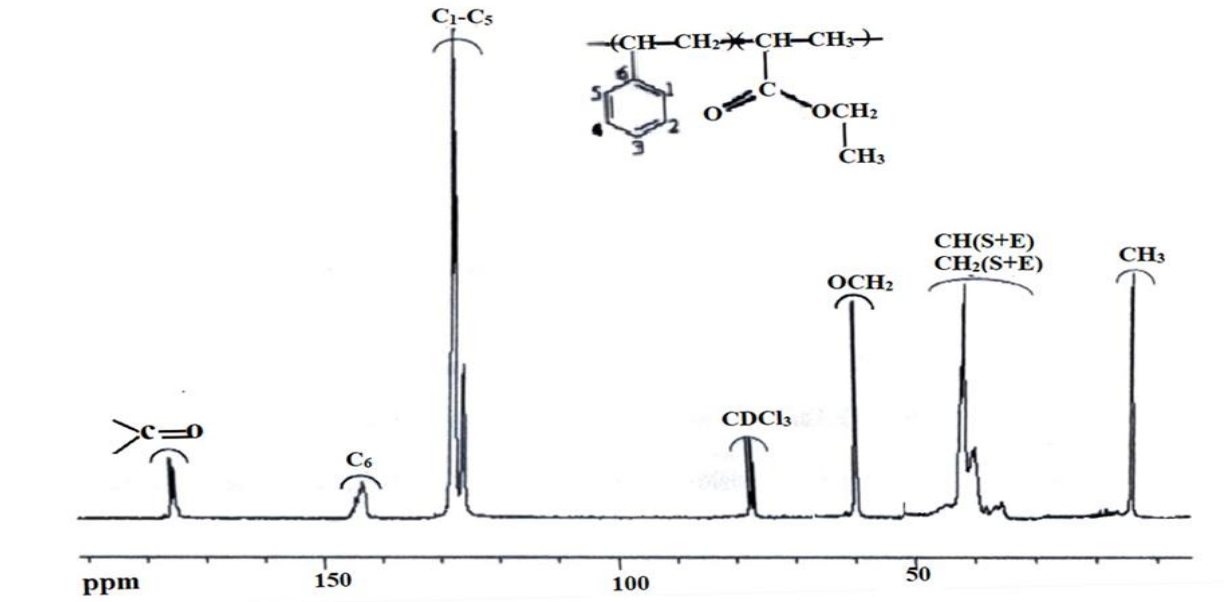

Figure 4. $^{13}C\{^{1}H\}$ NMR spectrum of the styrene/ ethyl acrylate copolymer (F_S=0.49) in $CDCl_3$ at 25°C

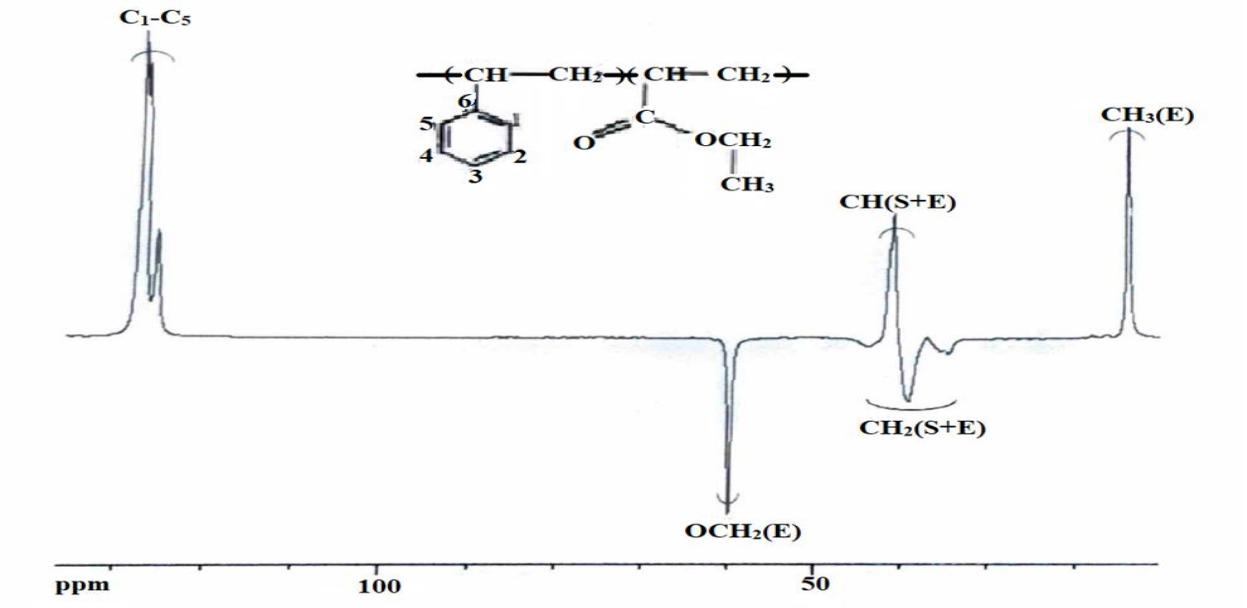

Figure 5. DEPT-135 NMR spectrum of the styrene/ ethyl acrylate copolymer (F_S=0.49) in $CDCl_3$ at 25°C

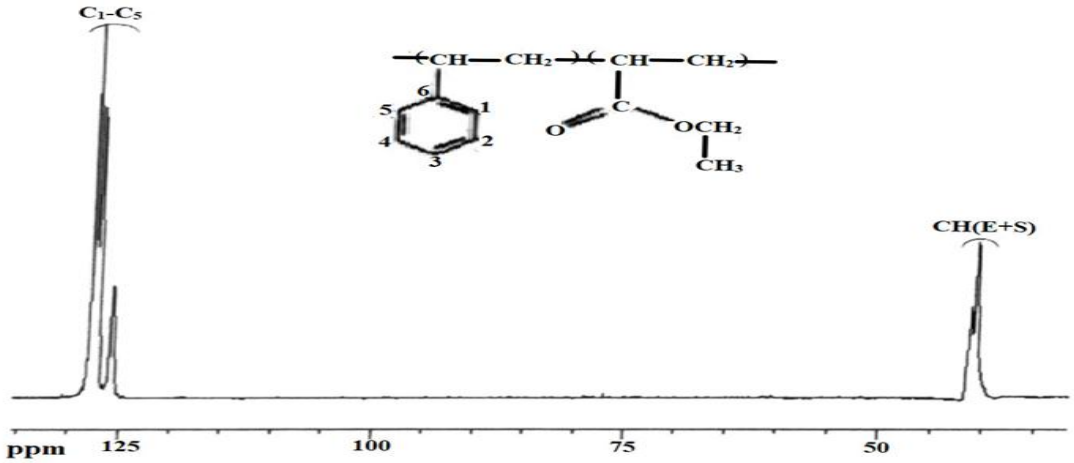

Figure 6. DEPT-90 NMR spectrum of the styrene/ ethyl acrylate copolymer (F_S=0.49) in $CDCl_3$ at 25°C

A comparative study of the carbonyl region across various S/E copolymer compositions and poly(ethyl acrylate) is depicted in Figure 7. Triad sequences corresponding to EEE, EES, and SES configurations were identified by analyzing changes in signal intensities as the styrene content increased. The quaternary carbon of the styrene unit's phenyl ring resonates between δ 142.4 and 146.6 ppm whereas the carbonyl carbon resonance of the E unit appears in the δ 174.23–178.57 ppm range. Expanded spectra showcasing different S/E copolymer compositions alongside polystyrene are provided in Figure 8.

By analyzing variations in copolymer composition and comparing the spectra with those of the corresponding homopolymers, the quaternary carbon resonance signals were assigned to specific triad sequences. The resonance signals in the δ 146.2–144.8 ppm range were attributed to the SSS triad, those between δ 144.8–143.6 ppm to the SSE triad, and signals around δ 143.6–142.4 ppm to the ESE triad. Quantitative calculations of these S- and E-centered triads were performed using the integrated areas of the respective resonance signals in the $^{13}C\{^1H\}$ NMR spectra of the copolymers. These results were further validated using

reactivity ratio calculations, showing strong agreement between both methods (Table 2).

Specific triad sequences were assigned to the quaternary carbon resonance signals by analyzing variations in copolymer composition and comparing the spectra with those of the corresponding homopolymers. The δ 146.2–144.8 ppm, δ 144.8–143.6 ppm and δ 143.6–142.4 ppm ranges were associated with the SSS, SSE and ESE triads. The relative proportions of these S- and E-centered triads were determined through quantitative analysis of the integrated areas of their respective resonance signals in the $^{13}C\{^{1}H\}$ NMR spectra. Reactivity ratio calculations were used to validate these findings, demonstrating a strong correlation between both approaches, as shown in Table 2.

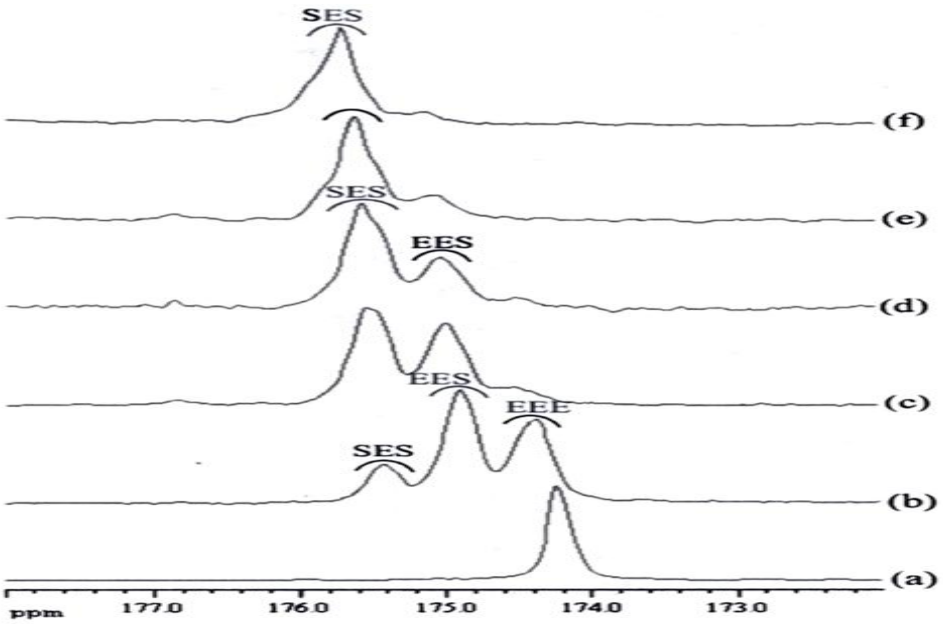

Figure 7. Expanded Carbonyl carbon of the E unit in the $^{13}C\{^{1}H\}$ NMR spectrum of the styrene/ethyl acrylate copolymer in $CDCl_3$ at 25°C: (a) poly(ethyl acrylate), (b) F_E=0.70, (c) F_E=0.51, (d) F_E=0.42, (e) F_E=0.31 and (f) F_E=0.20

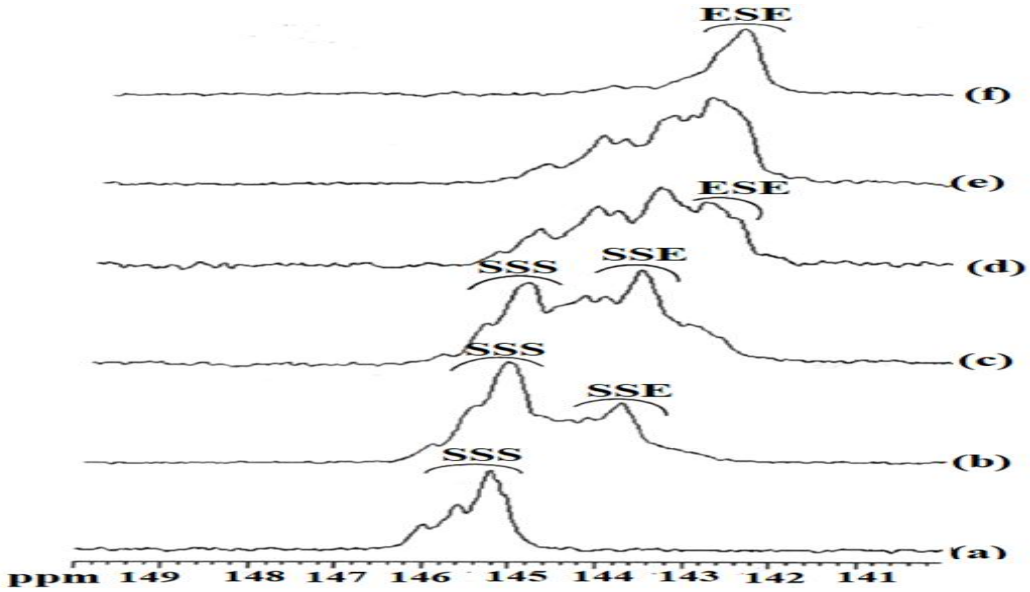

Figure 8. Expanded Quaternary carbon of the S unit in the $^{13}C\{^{1}H\}$ NMR spectrum of the styrene/ethyl acrylate copolymer in $CDCl_3$ at 25°C: (a) polystyrene, (b) F_S=0.80, (c) F_S=0.69, (d) F_S =0.58, (e) F_S=0.49 and (f) F_S=0.30

Table 2 Triad fractions calculated from the NMR spectra and reactivity ratios of S/E copolymers (<10% conversion)

Sample No.	Copolymer composition F_s	Triads	(a)	(b)
1.	0.80	SSS	0.67	0.63
		SSE	0.33	0.33
		ESE	0.00	0.04
		EEE	0.00	0.01
		EES	0.14	0.19
		SES	0.86	0.80
2.	0.69	SSS	0.43	0.41
		SSE	0.47	0.46
		ESE	0.10	0.13
		EEE	0.00	0.04
		EES	0.29	0.32
		SES	0.71	0.64
3.	0.58	SSS	0.23	0.24
		SSE	0.53	0.50
		ESE	0.24	0.26
		EEE	0.07	0.10
		EES	0.42	0.44
		SES	0.51	0.46
4.	0.49	SSS	0.14	0.15
		SSE	0.50	0.48
		ESE	0.36	0.37
		EEE	0.12	0.17
		EES	0.44	0.49
		SES	0.34	0.34
5.	0.30	SSS	0.00	0.04
		SSE	0.27	0.31
		ESE	0.73	0.65
		EEE	0.43	0.43
		EES	0.44	0.45
		SES	0.13	0.12

(a) Values of triad fractions determined from $^{13}C\{^1H\}$ NMR spectra based on resonance signals of quaternary and carbonyl carbons of S- and E-centered monomeric units of S/E copolymers and (b) Calculated triad fractions (r_S = 0.96, r_E = 0.47)

VI. 2D HSQC NMR STUDIES

The HSQC spectrum of S/E copolymers exhibits significant complexity, similar to that observed in Styrene/Methyl methacrylate (S/M) copolymers[38]. The CH and CH_2 groups of S and E acrylate units in the polymer backbone resonate distinctly in the ranges of δ 33.6–46.1 ppm and δ 1.17–1.90 ppm. The Figure 9 presents expanded 2D HSQC spectra for three distinct S/E copolymer compositions, corresponding to F_S values of 0.30, 0.49, and 0.80. The CH_2 carbon signals in S/E copolymers demonstrate sensitivity to compositional sequences. Variations in signal intensities with changes in copolymer composition allow for the classification of resonance signals within the CH_2 carbon region into dyad compositional sequences—EE, ES, and SS.

The EE dyad appears in the δ 33.6–37.0/1.17–1.90 ppm region and exhibits configurational sensitivity. The Cross peaks 1, 2, and 3, observed at δ 34.7/1.78, 35.2/1.58, and 34.9/1.44 ppm, respectively, correspond to the CH_2 dyad of the E unit, with peaks 1 and 3 assigned to the meso (m) configuration (EmE) and peak 2 attributed to the racemic (r) configuration (ErE), reflecting the presence of two non-equivalent protons.

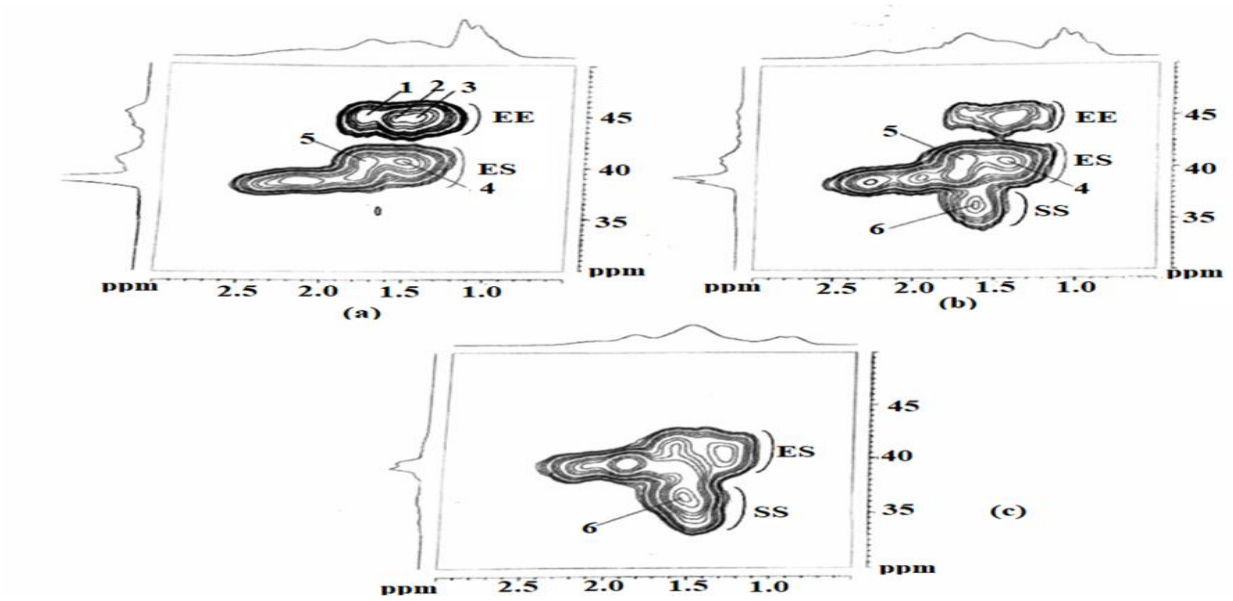

Figure 9. Expanded 2D HSQC NMR spectra of the three different compositions of S/E copolymers with Fs (a) = 0.30, (b) = 0.49 and (c) = 0.80 in $CDCl_3$ at 25ºC

The ES dyad region, spanning δ 37.8–42.5/1.2–1.9 ppm, and the SS dyad, appearing within δ 42–46/1.4–1.7 ppm, both exhibit additional splitting along the proton axis. Cross peaks 4, 5, and 6, at δ 39.3/1.56 ppm, 39.3/1.77 ppm, and 43.7/1.52 ppm, are assigned to the ErS, EmS, and SS dyads, respectively

VII. 2D TOCSY NMR STUDIES

The TOCSY spectra with F_S values of a = 0.30 and b = 0.69 in $CDCl_{3\ as}$ shown in Figure 10 distinctly exhibit three-bond, or vicinal, coupling between the CH_2 and CH protons. The peak positions, their corresponding assignments, and the associated couplings are detailed in Table 3.

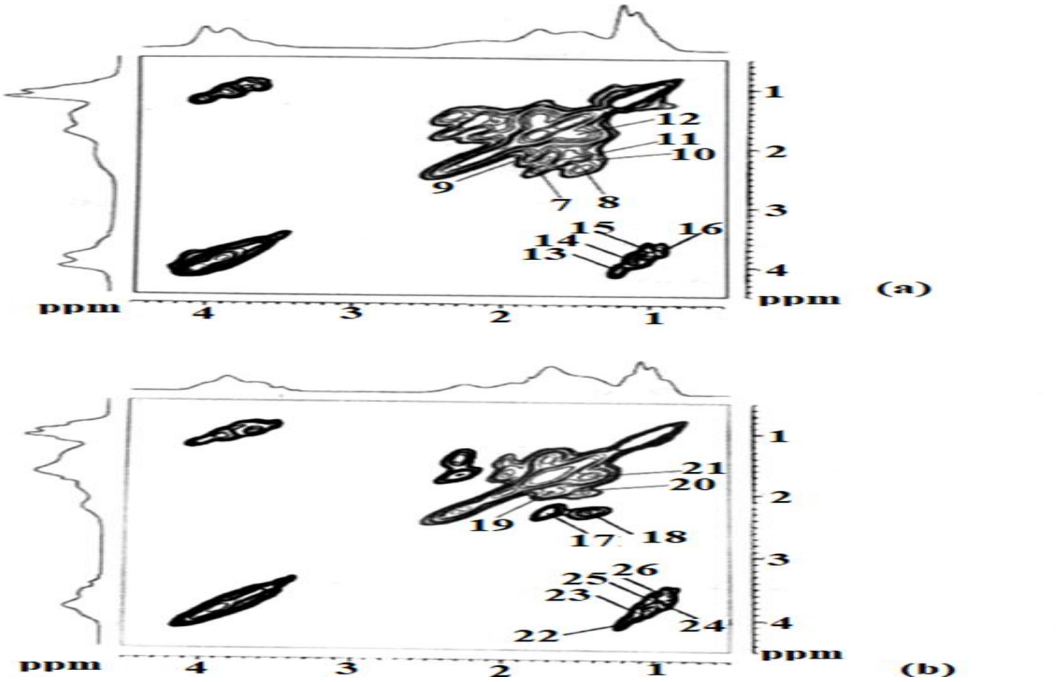

Figure 10. Expanded TOCSY spectra of two different compositions of S/E copolymers with F_s (a) = 0.30 and (b) = 0.69 in $CDCl_3$ at 25ºC

Table 3. ^{1}H-^{1}H cross correlation vicinal coupling between the non-equivalent methylene and methine protons in Styrene-Ethyl acrylate copolymers observed from 2D TOCSY spectra with F_S values of a = 0.30 and b = 0.69 in $CDCl_3$.

Correlation peak No.	Coupled protons Proton I	Proton II	Peak position 2D TOCSY;$^{1}H/^{1}H$; δ
7	CH_2 of EmE (Ha)	CH of EEE	1.78/2.36 1.44/2.36
8	CH_2 of EmE (Hb)	CH of EEE	1.44/2.36
9	CH_2 of EmE (Ha)	CH of EES	1.78/2.12 1.44/2.12
10	CH_2 of ErS	CH of EES	1.60/2.22
11	CH_2 of EmS (Hb)	CH of EES	1.44/2.12
12	CH_2 of EE (Ha) and ES (Ha)	CH_2 of EE (Hb) and ES (Hb)	1.46/1.78
13	OCH_2 of EEE	CH_3 of EEE	1.20/4.06
14	OCH_2 of EES	CH_3 of EES	1.10/3.89
15	OCH_2 of SrErS	CH_3 of SES	1.00/3.70
16	OCH_2 of SmErS	CH_3 of SES	0.91/3.76
17	CH_2 of EmS (Ha)	CH of SSE	1.70/2.30
18	CH_2 of EmS (Hb)	CH of SSE	1.44/2.30
19	CH_2 of SmS (Ha)	CH_2 of SmS (Hb)	1.70/1.97
20	CH_2 of SrS (Ha)	CH_2 of SrS (Hb)	1.42/1.97
21	CH_2 of ES (Ha)	CH_2 of ES (Hb)	1.38/1.70
22	OCH_2 of EEE	CH_3 of EEE	1.20/4.02
23	OCH_2 of EES	CH_3 of EES	1.10/3.85
24	OCH_2 of SrErS	CH_3 of SES	1.02/3.68
25	OCH_2 of SmErS	CH_3 of SES	0.93/3.62
26	OCH_2 of SmEmS	CH_3 of SES	0.90/3.72

VIII. CONCLUSION

The microstructure and sequence distribution of S/E copolymers were investigated using 1D and 2D NMR techniques in conjunction. These copolymers exhibited controlled molecular weights with narrow polydispersity. Our studies revealed that the spectra became more complex as the pendant group length increased. Reactivity ratios determined through the EVM method were found to be $r_S = 0.96$ and $r_E = 0.47$. Additionally, the triad distributions of carbonyl and quaternary carbon corresponded well with theoretical calculations derived from the reactivity ratios of the S/E copolymer system. Compositional and configurational sequences within the copolymers were accurately identified using advanced 2D NMR techniques, specifically HSQC and TOCSY experiments.

REFERENCES

[1] Mark, H. F.; Bikales, N. M.; Overberger, C. G. Encyclopedia of Polymer Sci and Engg; Wiley Interscience: New York 1989, 16, 242.

[2] Verma, N.; Aiswarya S.; Banerjee S. S. Polymer-Plastics Technology and Materials 2023, 62, 419.

[3] Tonelli, A. E.; Schilling, F. C. Acc Chem Res 1988, 14, 233.

[4] Dekkar, A. O.; Zimmermann, G. A. Ind Eng Chem Prod Res Develop 1962, 1, 23.

[5] Fei, G.; Zhou, Z.; Yang, C.; Li, S. Xie, P.; Journal of Applied Polymer Science, 2024, 141, 43.

[6] Eyann, L.; Rashid, S. M.; Musa, M. S. ; December 2024 Journal of Physics Conference Series 2907(1):012001, DOI: 10.1088/1742-6596/2907/1/012001

[7] Sarkar, A.; Jayram, R. V. Polymer science Series B, 2018, 60(5), 629.

[8] Taha, D. Y.; Ahmed, I. Z., J. Eng. Technol. Sci. 2025, 57(1), 93.

[9] Van Doremaele, G. H. J.; German, A. L.; de Vries, N. K.; Vander Velden, G. P. M. Macromolecules 1990, 23, 4206.

[10] Wang, S.; Poehlein, G. W. J Appl Polym Sci 1993, 49, 991.

[11] Randall, J. C. J Polym Sci Polym Phys Edn 1975, 13, 889.
[12] Sato, K.; Koinuma, H.; Hirai, H. Makromol Chem 1993, 4, 821.
[13] Djekabha, S.; Graillet, C.; Guillot, J. Eur Polym J 1988, 24, 109.
[14] Djekabha, S.; Guillot, J. Eur Polym J 1990, 26(9), 1017.
[15] Darricades, M. F. L.; Pichot, C.; Guillot, J.; Rios, L.; Cruz, M. A.; Guzman, C. Polymer 1986, 27, 889.
[16] Ito, K.; Yamashita, Y... J. Polym Sci: Part B: Polym Lett Ed 1965, 3, 637.
[17] Kobayashi, M. J Appl Polym Sci 1988, 35, 311.
[18] Vander Boomen, F. H. A. M.; Mecdijk, J.; Theones, D. Chem Engg Sci, 1996, 51, 2287.
[19] Khandelwal, D.; Hooda, S.; Brar, A. S.; and Shankar R. J. Polym. Research 2014, 21, 377.
[20] Khandelwal, D.; Hooda, S.; Brar, A. S.; and Shankar J. Mol. Struct. 2013, 1049, 99.
[21] Bovey, F. A. Chain Structure and Conformation of Macromolecules; Academic Press: New York, 1982.
[22] Randall, J. C. Polymer Sequence Distribution: Carbon I3C NMR Method; Academic Press: New York, 1977.
[23] Randall, J. C. NMR and Macromolecules: Sequence Dynamics and Domain Structure; ACS Symp Ser 247: Washington D. C.; 1984.
[24] Bovey, F. A.; Mirau, P. A. NMR of Polymers; Academic Press: New York, 1996.
[25] Matsuzaki, K.; Uryu, T.; Asakura, T. NMR Spectroscopy and Stereoregularity of Polymers; Japan Sci Soc Press: Tokyo, 1996.
[26] Hatada, K.; Kitayama, T. NMR Spectroscopy of Polymers; Springer-Verlag Berlin Heidelberg: Germany, 2004.
[27] Khandelwal, D.; Hooda s.; and Brar, A. S. J. Mol. Struct. 991 (2011) 24.
[28] Khandelwal, D.; Hooda, S.; Brar A. S. and Shankar, R. J. Mol. Struct. 1004 (2011) 121–130.
[29] Khandelwal, D.; Hooda, S.; Brar, A. S.; and Shankar, R. J. App. Polym. Sci. 126 (2012) 916.
[30] Khandelwal, D.; Hooda, S.; Brar A. S.; and Shankar R. J. Polym Sci Part A: Polym. Chem. 50 (2012) 3350.
[31] Khandelwal, D.; Kumar, V.; Misra, N. Sachdeva, S.; Rani, S. Verma, M.; Sahu, I. P.; Hooda, S. Applied Chemical Engineering Volume 6 Issue 1(2023) pg. 82.
[32] Khandelwal, D.; Kumar, V.; Singh, A.; Lal, S.; Kumari, R.; Hooda, S.; Rani, S.; Verma, M.; European Chemical Bulletin Vol. 12, Pg no. (2023) 2556-2567
[33] Jozaghkar, M.; Ziaee, F.; Azar, A. S.; Mehdipour-Ataei, S. Iranian Journal of polymer science and technology, 2023, 35(4), 393.
[34] Matyjaszewski, K.; Chem. Rev. 2022, 122, 1, 442.
[35] Matyjaszewski, K.; European Polymer Journal, 2024, 211, 113001.
[36] Kelen, T.; Tudos, F. J Macromol Sci Chem A9, 2, 1975.
[37] Debe, M. Sanyer, R. A.; Penlidis, A.; O'Driscoll, K. F.; Reilley, P. M. J. Polym Sci: Part A: Polym Chem 1991, 29, 703.
[38] Brar, A. S.; Puneeta. J. Polym. Sci. Part A: Polym. Chem. 2006, 44, 2076.